Structural study of the charge-density-wave modulation of isoelectronically doped $(Ta_{1-x}Nb_xSe_4)_2I$ $(0.1\% < x < 1.2\%)$

1998 J. Phys.: Condens. Matter 10 6505

(http://iopscience.iop.org/0953-8984/10/29/010)

J. Phys.: Condens. Matter **10** (1998) 6505–6514. Printed in the UK PII: S0953-8984(98)93213-1

Structural study of the charge-density-wave modulation of isoelectronically doped $(Ta_{1-x}Nb_xSe_4)_2I$ $(0.1\% < x < 1.2\%)$

H Requardt†‡, J E Lorenzo§+, R Currat‡, P Monceau†, B Hennion‖, H Berger¶ and F Levy¶

† Centre de Recherches sur les Très Basses Températures, CNRS, 38042 Grenoble, France
‡ Institut Laue–Langevin, 38042 Grenoble, France
§ Departement of Physics, Brookhaven National Laboratory, Upton, NY 11973-5000, USA
‖ Laboratoire Léon Brillouin, Centre d'Etude de Saclay, 91191 Gif-sur-Yvette, France
¶ Institut de Physique Appliquée, Ecole Polytechnique Fédérale de Lausanne, 1015 Lausanne, Switzerland

Received 9 April 1998

Abstract. We present a neutron and x-ray diffraction study of the charge-density-wave modulation wave vector of $(TaSe_4)_2I$ with isoelectronic Nb doping. In contrast to other charge-density-wave materials, like $NbSe_3$ and $K_{0.3}MoO_3$, Nb-doped $(TaSe_4)_2I$ reveals a change of the modulation wave vector with doping. This change corresponds to a shift of the satellite position towards the Brillouin-zone centre on a nominal doping level of 0.8% Nb being exceeded. On a 1.2% level of Nb doping being reached, strong satellite broadening is observed, indicating the onset of short-range charge-density-wave correlation. A recently derived phenomenological model of the phase transition in $(TaSe_4)_2I$, which accounts for changes in the modulation wave vector upon doping, is briefly discussed.

1. Introduction

The charge-density-wave (CDW) state observed in many quasi-one-dimensional compounds [1–3] is very sensitive to impurities and defects in the parent lattice, since the perturbing potential couples directly to the CDW phase φ. In an ideal crystal with an incommensurate modulation wave vector, Q_{mod}, of the CDW, the charge-density wave $\rho(r) = \rho_0 + \Delta\rho \sin(Q_{mod}r + \varphi)$ can freely slide through the system, since its phase is not fixed with respect to the parent lattice. In the presence of impurities or defect potentials the CDW phase is pinned, and the CDW is subject to deformations in the vicinity of such potentials.

A considerable amount of work has been concentrated on the investigation of the effects of different kinds of impurity and defect in CDW systems. The defects and impurities are introduced either by doping (isoelectronic or non-isoelectronic), or by irradiation damage. Most of the studies have focused on measurements of the electrical properties of the CDW systems upon doping, such as the threshold field and the non-linear resistivity above the threshold. The experimental results have been interpreted in terms of weak or strong pinning, the two limits treated with the theory of Lee, Rice and Anderson [4]. Most of the experimental work has been done on the compounds $NbSe_3$ (see, e.g., references [5–11]), TaS_3 [12, 13], the blue bronze $K_{0.3}MoO_3$ [14, 15] and $(TaSe_4)_2I$ [16, 17]. However, comparatively little work has been devoted to the investigation of the structural effects

+ Present address: Laboratoire de Cristallographie, CNRS, 38042 Grenoble, France.

0953-8984/98/296505+10$19.50

associated with doping. In the following section, we briefly review the experimental results available from previous studies.

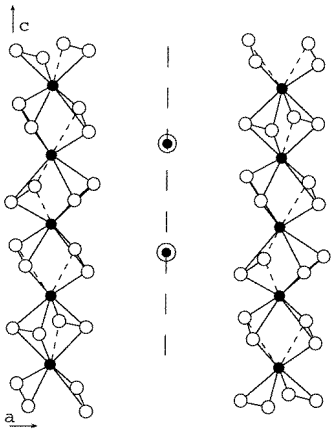

Figure 1. A schematic representation of the chain-like structure of $(TaSe_4)_2I$. The Ta (•) and Se (◯) atoms form chains of $(TaSe_4)_\infty$ separated by rows of I ions (⊙). This figure was taken from reference [3].

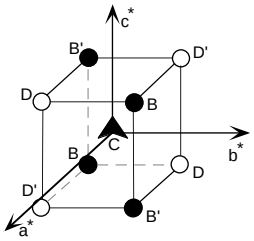

Figure 2. A sketch of the satellite positions (B, B′, D, D′) in the vicinity of a main reflection (C). Of the satellites in the vicinity of (HHL) reflections, the satellites B, B′ are more intense than satellites D, D′, with satellites B′, D′ weaker than satellites B, D. This figure was adapted from reference [22].

The system under study here is $(TaSe_4)_2I$ (space group $I422$), which is composed of parallel chains of $(TaSe_4)_\infty$ separated by rows of iodine ions (figure 1). The undoped compound undergoes a phase transition at $T_P = 260$ K into a CDW-modulated state. The low-temperature phase shows a set of eight satellite reflections at the positions $\boldsymbol{G} + (\pm\delta H, \pm\delta K, \pm\delta L)$ close to each main reflection $\boldsymbol{G} = (H, K, L)$ (figure 2). Typical values for pure $(TaSe_4)_2I$ are $\delta H = 0.045$ and $\delta L = 0.085$ (see, e.g., reference [3]). Studies of the conductivity of pure and isoelectronically Nb-doped samples (with up to 1.2% Nb) show a strong effect of doping on the temperature dependence of the resistivity ρ_{dc} [16, 17]: while the pure compound shows a sharp peak in the logarithmic derivative of the resistivity $\mathrm{d}(\ln(\rho_{dc}))/\mathrm{d}(1/T)$ on crossing the phase transition, this behaviour is progressively smeared out with increasing dopant concentration, eventually leading to the complete suppression of the resistivity anomaly associated with the transition (see figure 3). Similar behaviour has been observed in weakly tungsten-doped $K_{0.3}MoO_3$ by Schneemeyer *et al* [14]. Recently, Saint-Paul *et al* [18] also observed such a behaviour in a study of ultrasonic properties and

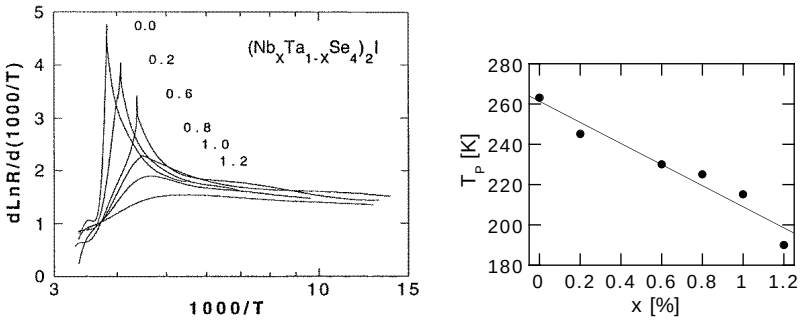

Figure 3. Left: The temperature dependence of the resistivity derivative $\mathrm{d}(\ln(\rho_{dc}))/\mathrm{d}(1/T)$ for isoelectronically doped $(TaSe_4)_2I$: $x(\mathrm{Nb}) = 0, \ldots, 1.2\%$. This figure was adapted from reference [17]. Right: the dependence of the transition temperature T_P on the Nb doping level in $(TaSe_4)_2I$. T_P is defined as the maximum of $\mathrm{d}(\ln(\rho_{dc}))/\mathrm{d}(1/T)$. The data were taken from reference [17].

the thermal expansion of $(TaSe_4)_2I$ doped with Nb up to a nominal concentration of 1.2%. In the pure system the sound velocity corresponding to the elastic constant C_{44} shows a sharp anomalous softening in the vicinity of the phase transition temperature. With doping, this anomaly is reduced and it finally disappears at a doping level of 1.2% Nb. As in the case of the electrical conductivity data, both the transition temperature deduced from the dip of the sound velocity anomaly and the amplitude of the anomaly are reduced with increasing doping level.

In this paper we present measurements of the dependence of the satellite peak position, on the amount of isoelectronic Nb dopant present. Several samples of $(Ta_{1-x}Nb_xSe_4)_2I$ were studied, prepared in two different series of growth batches, with doping levels of nominally 0.1% up to 1.2% Nb ($x = 0.001, \ldots, 0.012$). Contrary to the cases for other CDW systems, isoelectronic doping of $(TaSe_4)_2I$ leads not only to the expected reduction of the CDW correlation length, even at weak doping levels, but also to a change in the CDW modulation wave vector, above a threshold dopant concentration.

2. Previous structural studies of doped CDW systems

Studies of the structural effects of doping have mostly been concerned with the reduction of the phase–phase correlation length of the CDW: measurements have been performed on isoelectronically (Rb, W)-doped $K_{0.3}MoO_3$ by Tamegai *et al* [15], on hydrogen-doped $NbSe_3$ by Thorne *et al* [20] and on isoelectronically (Ta-) doped $NbSe_3$ by Sweetland *et al* [21]. These studies reveal a broad range of sensitivity to the different kinds of doping atom: strong hydrogen doping (up to 7%) has very little effect on the CDW threshold field and the phase transition temperature in $NbSe_3$ [20], whereas doping with as little as 0.5% Ta significantly lowers the transition temperature T_P and decreases the CDW phase–phase correlation length [21, 9]. Comparable sensitivity is found for W-doped $K_{0.3}MoO_3$ [15] where the introduction of a very small amount of tungsten significantly lowers the transition temperature and strongly reduces the CDW correlation length. In contrast, doping with Rb, even up to a level of 50%, has very little effect either on T_P or on the superstructure correlation length.

This sensitivity to Ta in $NbSe_3$ and to W in $K_{0.3}MoO_3$ may be understood in terms of Ta and W entering the metallic chains –Nb–Nb– and –Mo–Mo–, respectively, thus perturbing

the quasi-one-dimensional electronic subsystem. In contrast, hydrogen in $NbSe_3$ and Rb in $K_{0.3}MoO_3$ occupy interstitial positions (the alkaline ions are located 'interstitially' between the molybdenum–oxygen slabs in $K_{0.3}MoO_3$) and are thus expected to have comparably little effect on the CDW.

Among the very few studies of the effect of doping on Q_{mod}, measurements have been performed on blue bronze doped with *non-isoelectronic* vanadium, $K_{0.3}V_xMo_{1-x}O_3$ ($x \approx 0.02$), by Girault *et al* [24], yielding a change in the satellite position between the pure system and the doped system. Accompanying this change in Q_{mod}, a significant reduction of the phase–phase correlation length is observed, as seen in the strongly broadened satellite reflections of the doped compound.

Recently, Rouzière *et al* [23] reported measurements on titanium-doped $NbSe_3$ ($Ti_xNb_{1-x}Se_3$) with doping levels of $x = 0.01$ and 0.05. As for the blue bronze, changes in satellite position have been found with this *non-isoelectronic* doping. The measured CDW modulation wave vectors found upon doping are summarized in table 1.

So far, *no* changes of the CDW modulation wave vector due to *isoelectronic* doping have been reported.

Table 1. Satellite positions $(0, \delta K, 0)$ for Ti-doped $NbSe_3$ and $(0, \delta K, 0.5)$ for V-doped $K_{0.3}MoO_3$ as observed by Rouzière *et al* [23] and Girault *et al* [24].

$Nb_{1-x}Ti_xSe_3$, reference [23]		$K_{0.3}Mo_{1-x}V_xO_3$, reference [24]	
Nominal doping	δK	Nominal doping	δK
Pure ($x = 0$)	0.241	Pure ($x = 0$)	0.749
$x = 0.01$	0.227	$x = 0.02$	0.685
$x = 0.05$	0.20		

3. Experimental procedure

Measurements on samples with Nb doping levels of 0.1%, 0.4%, 0.8% and 1.2% (samples A, B, C and D, respectively) were carried out on the cold-neutron three-axis spectrometer 4F1 at the Laboratoire Léon Brillouin (LLB) (Saclay, France) using an incident neutron energy of $E_i = 5$ meV ($k_i = 1.55$ Å^{-1}, $\lambda = 4.05$ Å). The rod-shaped samples, of typical sizes 8–20 mm in length and 2–4 mm in diameter, were mounted in a closed-cycle refrigerator. The samples were oriented so as to have an $(H0L)$ horizontal scattering plane. This orientation allows one to study the two components δH and δL of the satellite wave vector $(\pm\delta H, \pm\delta H, \pm\delta L)$ (see figure 2) with the high q-resolution available in the scattering plane. The relaxed vertical resolution is used to integrate over the pair of satellites $(H, \pm\delta H, L)$ situated below and above the scattering plane.

In our measurements, the satellite intensities were monitored at several temperatures below T_P at the positions $(2 \pm \delta H, 0, 4 \pm \delta L)$ in the vicinity of the (204) Bragg reflection.

Depending upon resolution/intensity requirements, we used collimations of 60′–25′–40′–60′ and 15′–25′–20′–20′. The former set-up yielded an experimental resolution (FWHM) of $\Delta q_{(001)} = 0.020$ Å^{-1}, $\Delta q_{(100)} = 0.013$ Å^{-1} in the scattering plane and $\Delta q_{(010)} = 0.07$ Å^{-1} vertically. The corresponding values using tighter collimations (second set-up) are $\Delta q_{(001)} = 0.014$ Å^{-1}, $\Delta q_{(100)} = 0.008$ Å^{-1} and $\Delta q_{(010)} = 0.065$ Å^{-1}. These values were deduced from scans across the Bragg reflection (204) and include the effect of the sample mosaicity.

Additional samples from different growth batches but with similar nominal doping levels, 0.4%, 0.8% and 1.2% (samples E, F and G, respectively), were studied at low temperature (10 K) using elastic neutron scattering ($E_i = 5$ meV) on the cold-neutron three-axis spectrometer H9 at the High Flux Brookhaven Reactor (HFBR). The samples were mounted in a closed-cycle refrigerator with an $(H\,H\,L)$ horizontal scattering plane, allowing one to monitor satellites in the vicinity of the (224) main reflection. The relaxed vertical resolution was used to integrate over the pair of satellite reflections at $(2\mp\delta H, 2\pm\delta H, 4-\delta L)$ and $(2\mp\delta H, 2\pm\delta H, 4+\delta L)$, those at $(2\pm\delta H, 2\pm\delta H, 4-\delta L)$ and $(2\pm\delta H, 2\pm\delta H, 4+\delta L)$ being extinct. The samples labelled E, F and G were also studied using the high-resolution x-ray diffractometer X22B at the National Synchrotron Light Source (NSLS-Brookhaven) with an incident photon energy of $E_i = 8.02$ keV. The satellite reflections near the (400), (440) and (554) Bragg reflections were studied.

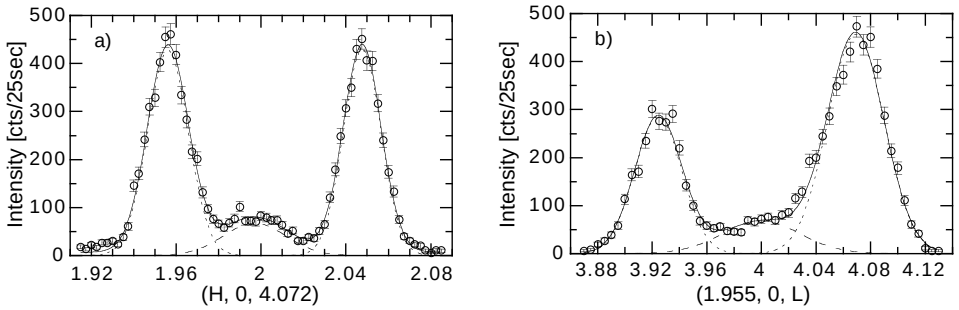

Figure 4. Sample A ($(TaSe_4)_2I$ with 0.1% Nb); satellites near the (204) main reflection. (a) Satellites at $(\pm\delta H, \pm\delta H, +\delta L)$ scanned along $\boldsymbol{a}^*$. (b) Satellites at $(-\delta H, \pm\delta H, \pm\delta L)$ scanned along $\boldsymbol{c}^*$. The intensity distributions centred around $H = 2$ and $L = 4$ are ascribed to contributions from inelastic scattering from transverse acoustic phonons. ($T = 21.9$ K.)

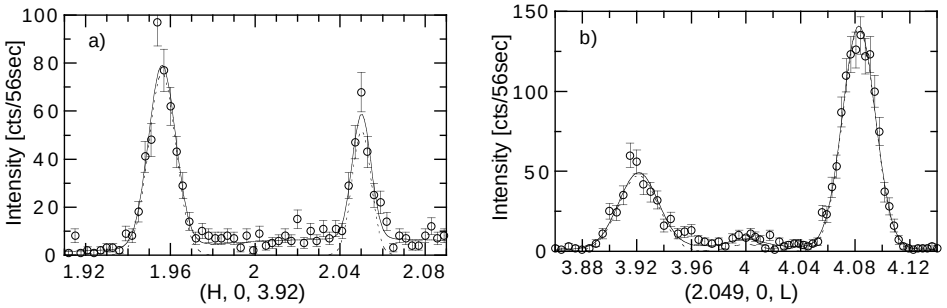

Figure 5. Sample C (0.8% Nb); satellites near the (204) main reflection. (a) Satellites at $(2\pm\delta H, 2\pm\delta H, 4-\delta L)$ scanned along $\boldsymbol{a}^*$. (b) Satellites at $(2+\delta H, 2\pm\delta H, 4\pm\delta L)$ scanned along $\boldsymbol{c}^*$. ($T = 22.1$ K.)

4. Results

Figures 4 and 5 show scans along the directions $\boldsymbol{a}^*$ and $\boldsymbol{c}^*$ across pairs of satellites for samples A (0.1%) and C (0.8%) as obtained using the 4F1 neutron spectrometer. The satellite profiles only appear sharper in figure 5 than in figure 4 due to different instrumental

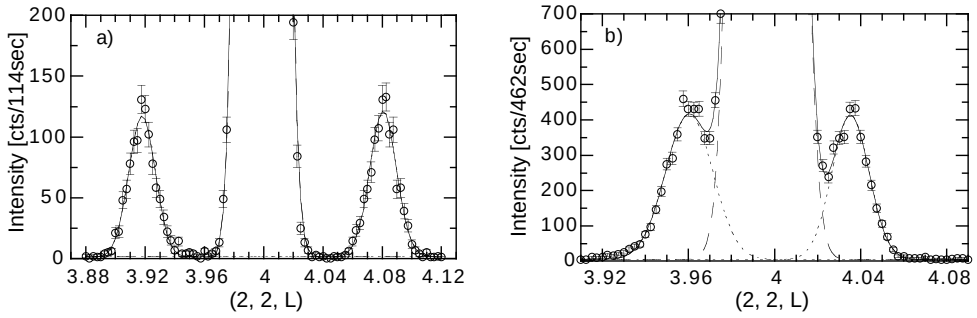

Figure 6. The satellites at $(\mp\delta H, \pm\delta H, \pm\delta L)$ near the (224) main reflection of $(TaSe_4)_2I$ scanned along $\boldsymbol{c}^*$. (a) Sample F (0.8% of Nb). (b) Sample G (1.2% Nb). The strong peak centred around $L = 4$ corresponds to the (224) Bragg reflection. ($T = 10$ K.)

resolution conditions. The low-resolution scans (figures 4(a) and 4(b)) show contributions centred around $H = 2$ and $L = 4$, respectively. These contributions correspond to inelastic scattering within the energy window of the three-axis spectrometer (55 GHz FWHM) from low-frequency transverse acoustic (TA) phonons. We note that in $(TaSe_4)_2I$ all TA branches associated with the elastic constant C_{44} are very soft. This applies to the TA modes propagating in the basal plane ($\boldsymbol{a}^*$, $\boldsymbol{b}^*$) and polarized along $\boldsymbol{c}^*$, and to the doubly degenerate TA branch propagating along $\boldsymbol{c}^*$ [19, 25]. Figure 6 shows scans along the chain direction $\boldsymbol{c}^*$ across pairs of satellites for samples F (0.8% Nb; figure 6(a)) and G (1.2% Nb; figure 6(b)), performed on the H9 neutron spectrometer. The intense peak at $L = 4$ corresponds to the (224) Bragg reflection. Notice the reduced value of the component δL of the satellite peaks in sample G compared to the less doped samples E and F.

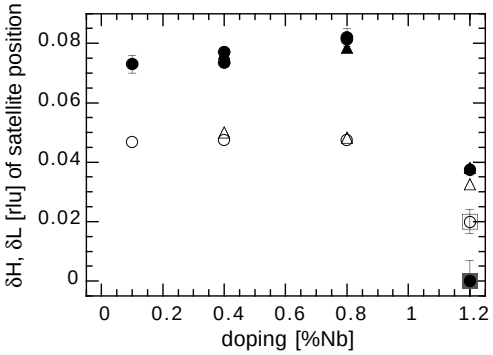

Figure 7. The components δH (open symbols) and δL (full symbols) of the satellite wave vector for doping levels from 0.1% up to 1.2% Nb. Circles: this work (neutrons); triangles: this work (x-rays). Squares: data from reference [25].

The values of δH and δL for the various samples investigated are shown in figure 7 together with data from earlier neutron measurements by Lorenzo [25]. Up to a nominal doping level of 0.8%, the satellite positions remain unchanged at $\delta H = 0.048$ and $\delta L = 0.071$–0.082, within the range of values reported for the pure compound (see, e.g., references [3] and [22]). For doping levels up to 0.8% Nb, the observed satellite profiles reveal a small but progressive broadening with doping, indicating a continuous

decrease of the phase–phase coherence length of the CDW.

The temperature dependences of the satellite intensities are very similar for the samples with 0.1% and 0.4% Nb (samples A and B), and for the pure compound [25]. From the broadening of the satellite profiles with increasing temperature, the phase transition temperature of the 0.1% Nb sample (sample A) is estimated to be about 240 K. That of the 0.4% Nb sample (sample B) can be estimated to be 230 K. For 0.8% Nb (samples C and F), the satellite intensities show a much smoother temperature dependence, closer to that observed earlier for a 1.2% Nb sample [25]. From the temperature dependence of the width of the satellite along H, one can estimate a phase transition temperature of about 220 K. The tendency of the transition temperature to decrease with increasing Nb content is in agreement with the behaviour found in resistivity measurements [16, 17] (figure 3) and in studies of the ultrasonic properties [18] of similarly doped samples.

At a nominal doping level of 1.2%, the satellite positions are shifted considerably closer to the main reflection: for sample G one finds $\delta H = 0.0325$, $\delta L = 0.038$ (figure 6(b)). The satellite peak profiles are broadened, but still indicate a well defined superstructure. For sample D, with nominally the same Nb doping level, the effect is even more dramatic: the component δH is reduced to $\delta H = 0.02$, with the intensity profiles showing a strong broadening, even far below the phase transition ($T = 22$ K, $T_P \approx 200$ K [16, 17]). Along the chain direction, the scattering is only observable as a broad intensity distribution centred around $\delta L = 0$. Taking the finite q-resolution along L into account, one estimates the intrinsic q-extension of this diffuse scattering to be $\simeq 0.07\boldsymbol{c}^*$. These results are in very close agreement with earlier results given by Lorenzo *et al*, who also find $\delta H = 0.02$ and $\delta L = 0$, and an intrinsic width along $\boldsymbol{c}^*$ of about $0.1\boldsymbol{c}^*$ [25]. The different behaviours observed for the *nominally identical* samples G and D could be due to small differences in the *effective* doping levels for samples coming from different growth batches. The magnitude of the changes in the superstructure wave vector indicates an effective doping level of sample G intermediate between those of samples C or F and that of sample D.

The intrinsic q-widths of the intensity distribution observed around $\delta H = 0.02$, $\delta L = 0$ for sample D indicate correlation lengths of about 25 Å along the chains and about 35 Å perpendicular to the chains. This corresponds to a correlation volume of about $3.7 \times 3.7 \times 2$ unit cells. With a nominal Nb concentration of 1.2% this corresponds to one Nb impurity atom per correlation volume. This suggests that the Nb impurities act as strong pinning centres and that the observed intensity distribution arises from short-range CDW correlations centred on the Nb impurities, rather than from remnants of a coherent superstructure. This interpretation is in agreement with the observation of a nearly or completely suppressed phase transition at this doping level, as reported in references [16, 18].

5. Discussion

The dramatic change of the CDW modulation wave vector of $(TaSe_4)_2I$ with the highest doping level is quite surprising, since so far studies on *isoelectronically* doped CDW systems did not report any influence of doping on the CDW satellite position.

Indeed such effects are characteristic of *non-isoelectronic* doping, as in Ti-doped $NbSe_3$ [23] and V-doped $K_{0.3}MoO_3$ [24] (see section 2).

For non-isoelectronic doping, the change of the CDW modulation wave vector is understood, in a simple rigid-band picture, as resulting from the change in the conduction electron density induced by the dopant ions. This change is in turn reflected in a change of the conduction electron Fermi wave vector k_F.

Such a mechanism is certainly not applicable here: even if we assume that, somehow, the

conduction electron concentration is modified by Nb doping, one would expect an increase rather than a decrease in the CDW wave vector, since for the isomorphous compound $(NbSe_4)_2I$ one gets $\delta H = 0.065$ and $\delta L = 0.159$ (Fujishita *et al* [26]).

This puzzling behaviour illustrates the non-standard character of the Peierls instability for $(TaSe_4)_2I$ and $(NbSe_4)_2I$, as compared to prototype CDW systems such as KCP, $NbSe_3$ and $K_{0.3}MoO_3$. On one hand the electrical conductivity in $(TaSe_4)_2I$ has a strong quasi-one-dimensional character and the existence of a CDW ground state below T_P is well established. On the other hand one observes not a giant Kohn anomaly but just very limited softening of a TA branch and no softening in the low-frequency optic branches (Lorenzo *et al* [25]). The CDW modulation wave vector has three irrational components, none of which shows any temperature dependence [25], in contrast to the cases for $NbSe_3$ (Moudden *et al* [29, 30]) and $K_{0.3}MoO_3$ [24]. Finally, the correlation lengths of the pre-transitional fluctuations are nearly isotropic in $(TaSe_4)_2I$ [31] and $(NbSe_4)_2I$ [26], in contrast to the high anisotropy of the electrical transport properties, which is again different from the case for other CDW compounds ($NbSe_3$ [29, 30], KCP [27, 32] and $K_{0.3}MoO_3$ [33]) which show strongly anisotropic pre-transitional fluctuations.

All of the above experimental evidence points to the need for a more sophisticated model to describe the Peierls mechanism in $(TaSe_4)_2I$ and $(NbSe_4)_2I$. Lorenzo *et al* [28, 25] have recently proposed a Landau–Ginzburg (LG) approach which takes the combined electronic and elastic properties of $(TaSe_4)_2I$ into account, as well as the detailed space group symmetry of the parent lattice. In this model the ordering variable is a combination of optic normal coordinates corresponding to the in-chain tetramerization of the Ta ions, with accompanying readjustment of the Se^{2-} dimers. The LG free-energy functional is written as $F = F_\eta + F_E + F_C$. There F_η stands for the free energy connected with the tetramerization variables, F_E for the elastic energy and F_C for the coupling between the optic tetramerization modes and the elastic deformations. The minimization procedure leads to a modulated low-temperature state for which the modulation wave-vector components $(\delta H, \delta H, \delta L)$ can be obtained, in principle, in terms of the various free-energy coefficients. These coefficients include the gradient coefficients for the optic variables, the elastic constants and the coefficients of coupling between the optic and elastic variables.

Doping can be viewed as introducing defects into the lattice. The presence of a finite concentration of defects is expected to renormalize at least some of the above coefficients and hence to affect the equilibrium values of δH and δL. The observed decrease of δH and δL with doping could then be correlated with an increase in the magnitude of the optic-mode gradient coefficients.

The above phenomenological model offers a framework within which a number of experimental observations, including that of the evolution of the CDW wave vector with doping, can be discussed. It is unlikely, however, that such a model can account for an abrupt change in the CDW wave vector at some finite Nb concentration (∼1%) [34]. This indicates the need for a more systematic study of the CDW satellite position for doping levels around 1%. A crucial prerequisite for future studies along these lines is the precise determination of the actual dopant concentration in a given sample, a point which has not been dealt with satisfactorily so far.

6. Conclusion

We have presented elastic neutron scattering results on the evolution of the CDW satellite positions in the compound $(TaSe_4)_2I$ with Nb doping. The results show a dramatic dependence of the satellite position around a doping level of about 1%

Nb which is unexpected for systems undergoing a simple Peierls transition, and in contrast to results reported for other isoelectronically doped CDW systems. A recently developed phenomenological model offers a mechanism for the doping dependence of the superstructure reflections of $(TaSe_4)_2I$ in terms of a defect-perturbed lattice. Further experimental data are required for doping concentrations near 1% and above.

Acknowledgments

We thank P Boutrouille for his kind assistance during the experiment at LLB/Saclay. H Requardt acknowledges financial support from the French Ministry of Education and Research (MESR). The work at Brookhaven National Laboratory (BNL) was supported by the US Department of Energy under contract No DE-AC02-76CH00016.

References

[1] Grüner G 1994 *Density Waves in Solids (Frontiers in Physics 89)* (New York: Addison Wesley)
[2] *ECRYS '93* 1993 *J. Physique Suppl.* I **3**
[3] Monceau P 1985 *Electronic Properties of Inorganic Quasi-one-dimensional Compounds* ed P Monceau (Dordrecht: Reidel) p 139
[4] Lee P A, Rice T M and Anderson P M 1973 *Phys. Rev. Lett.* **31** 462
Lee P A, Rice T M and Anderson P M 1974 *Solid State Commun.* **14** 703
Fukuyama H and Rice T M 1978 *Phys. Rev.* B **17** 535
Lee P A and Rice T M 1979 *Phys. Rev.* B **19** 3970
[5] Brill J W, Ong N P, Eckert J C, Savage J W, Khanna S K and Somoano R B 1981 *Phys. Rev.* B **23** 1517
[6] Monceau P 1982 *Physica* B **109+110** 1890
[7] Coleman R V, Everson M P, Lu Hao-An and Johnson A 1990 *Phys. Rev.* B **41** 460
[8] Maeda A and Uchinokura K 1990 *J. Phys. Soc. Japan* **59** 234
[9] DiCarlo D A, McCarten J, Adelman T L, Maher M and Thorne R E 1990 *Phys. Rev.* B **42** 7643
[10] McCarten J, DiCarlo D A, Maher M P, Adelman T L and Thorne R E 1992 *Phys. Rev.* B **46** 4456
McCarten J, Maher M P, Adelman T L and Thorne R E 1989 *Phys. Rev. Lett.* **63** 2841
[11] Dai Z, Slough C G and Coleman R V 1992 *Phys. Rev.* B **45** 9469
[12] Hsieh Pei-Ling, de Czito F, Janossy A and Grüner G 1983 *J. Physique* **44** C3 1753
[13] Rashid M H, Sellmyer D J and Kirby R D 1984 *Phys. Rev.* B **29** 5398
[14] Schneemeyer L F, DiSalvo F J, Spengler S E and Waszczak J V 1984 *Phys. Rev.* B **30** 4297
[15] Tamegai T, Tsutsumi K and Kagoshima S 1987 *Synth. Met.* **19** 923
[16] Kim Tae Wan, Donovan S, Grüner G and Philipp A 1991 *Phys. Rev.* B **43** 6315
[17] Chen J and Monceau P 1994 unpublished
[18] Saint-Paul M, Holtmeier S, Britel R, Monceau P, Currat R and Levy F 1996 *J. Phys.: Condens. Matter* **8** 2021
[19] Lorenzo J E, Currat R, Dianoux A J, Monceau P and Levy F 1996 *Phys. Rev.* B **53** 8316
[20] Thorne R E, Adelman T L, McCarten J, Maher M and McDowell A 1989 *Phys. Rev.* B **40** 4205
[21] Sweetland E, Tsai C-Y, Wintner B A, Brock J D and Thorne R E 1990 *Phys. Rev. Lett.* **65** 3165
[22] Lee K-B, Davidov D and Heeger A 1985 *Solid State Commun.* **54** 673
[23] Rouzière S, Ravy S and Pouget J P 1995 *Synth. Met.* **70** 1259
[24] Girault S, Moudden A H, Pouget J P and Godard J M 1988 *Phys. Rev.* B **38** 7980
[25] Lorenzo J E, Currat R, Monceau P, Hennion B, Berger H and Levy F 1988 *J. Phys.: Condens. Matter* **10** 5039
[26] Fujishita H, Sato M, Sato S and Hoshino S 1985 *J. Phys. C: Solid State Phys.* **18** 1105
[27] Carneiro K, Shirane G, Werner S A and Kaiser S 1976 *Phys. Rev.* B **13** 4258 and references therein
[28] Lorenzo J E, Monceau P, Currat R, Requardt H and Levy F 1998 *Physica* B **244** 91
[29] Moudden A H, Axe J D, Monceau P and Levy F 1990 *Phys. Rev. Lett.* **65** 223
[30] Moudden A H, Vasiliu-Doloc L, Monceau P and Levy F 1993 *J. Physique* I *Suppl. J. Physique Coll.* IV **3** C2 121
[31] Requardt H, Kalning M, Burandt B, Press W and Currat R 1996 *J. Phys.: Condens. Matter* **8** 2327
[32] Lynn J W, Iizumi M, Shirane G, Werner S A and Saillant R B 1975 *Phys. Rev.* B **12** 1154

[33] Girault S, Moudden A H and Pouget J P 1989 *Phys. Rev.* B **39** 4430
[34] Recent preliminary electron diffraction measurements [35] suggest a modified room temperature structure of $(Ta_{1-x}Nb_xSe_4)_2I$ at a doping level of $x = 1.2\%$.
[35] Audier M, private communication